CrossMark

sciendo Applied Mathematics and Nonlinear Sciences 4(1) (2019) 255–266

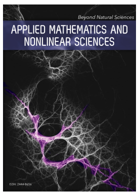

Applied Mathematics and Nonlinear Sciences

https://www.sciendo.com

Steady flow of a power law fluid through a tapered non-symmetric stenotic tube

Riaz Ahmad[1]†, Asma Farooqi[1], Jiazhong Zhang[1], Nasir Ali[2]

[1] School of Energy and Power Engineering, Xi'an Jiaotong University, Xi'an, 710049, China

[2] Department of Mathematics and statistics, International Islamic University, Islamabad, Pakistan

Submission Info

Communicated by Jose Maria Amigo Garcia
Received October 31st 2018
Accepted December 19th 2018
Available online June 28th 2019

Abstract

A steady flow of a power law fluid through an artery with a stenosis has been analyzed. The equation governing the flow is derived under the assumption of mild stenosis. An exact solution of the governing equation is obtained, which is then used to study the effects of various parameters of interest on axial velocity, resistance to flow and shear stress distribution. It is found that axial velocity increases while resistance to flow decreases when going from shear-thinning to shear-thickening fluid. Moreover, the magnitude of shear stress decreases by increasing the tapering parameter. This problem was already addressed by Nadeem et al. [14], but the results presented by them were erroneous due to a mistake in the derivation of the governing equation of the flow. This mistake is highlighted in the "Formulation of the Problem" section.

Keywords: Stenotic tube; Steady flow; Power law model; Steady flow; Non symmetric.
AMS 2010 codes: 37A60, 37D40 .

1 Introduction

Blood flow through stenotic arteries is a subject of recent investigation from the past few decades. Development of stenosis in the arteries is one of the leading causes of circulatory disorder. In medical terms, "narrowing of anybody passage" is called stenosis. This growth is abnormal and unnatural in the thickness of arterial wall that produces at different positions in the cardiovascular system under particular conditions. It has been observed that stenosis is due to the close association of the conditions of flow in the blood vessels. Rindfleish [1] and Nazemi et al. [2] analyzed that wall shear stress is a normal factor in the growth of atherosclerotic lesions. Caro et al. [3] suggested that atheroma appears in the low shear stress region while in view of Fry [4, 5] endothelial damage is caused by high wall shear stress. Once the stenosis is formed, it is quite clear that the flow characteristics in its vicinity may be significantly altered. The knowledge of various flow parameters in the stenotic artery such as the pattern of velocity, the rate of flow and the stresses is quite helpful to develop bio-medical instruments for bio-medical engineers for treating such modalities.

†Corresponding author
Email address: riazgill@stu.xjtu.edu.cn

sciendo ISSN 2444-8656 doi:10.2478/AMNS.2019.1.00022 sciendo

In recent years, the use of non-Newtonian models in studies regarding blood flow through stenotic arteries has considerably increased. In these studies the blood is represented by various non-Newtonian models such as Casson's model [6], power law model [7–9], micropolar model [10, 11], Sisko model [12] and Herschel–Bulkley model [13] etc. More recently Nadeem et al. [14] performed a study on blood flow through stenotic artery using the power law model. Unfortunately, they did not choose the proper sign preceding the magnitude of the rate of deformation tensor in their study, and thus they provided erroneous results. This motivated us to look into their problem and rectify the results presented by them. The details are included in this article. A detailed derivation of the governing equation is presented in Section 2. The mistake done by Nadeem et al. [14] is also pointed out here. An exact solution of the equation is obtained in Section 3. Section 4 consists of results and discussion. Conclusion of the paper is given in Section 5.

2 Formulation of the Problem

We consider an incompressible flow of power law fluid through a tube of length L. We choose the cylindrical coordinate system (r,θ,z) such that u, v and w are the velocity components in radial, azimuthal and axial directions, respectively, to analyze this flow. The governing equations of steady incompressible flow of a power law fluid are

$$\frac{\partial u}{\partial r}+\frac{u}{r}+\frac{\partial w}{\partial z}=0, \tag{1}$$

$$\rho\left(u\frac{\partial}{\partial r}+w\frac{\partial}{\partial z}\right)u=-\frac{\partial p}{\partial r}+\frac{1}{r}\frac{\partial}{\partial r}(rS_{rr})+\frac{\partial}{\partial z}(S_{rz})-\frac{S_{\theta\theta}}{r}, \tag{2}$$

$$\rho\left(u\frac{\partial}{\partial r}+w\frac{\partial}{\partial z}\right)w=-\frac{\partial p}{\partial z}+\frac{1}{r}\frac{\partial}{\partial r}(rS_{rz})+\frac{\partial}{\partial z}(S_{zz}), \tag{3}$$

where ρ is the density and p is the pressure of the blood.
The extra stress tensor **S** for power law fluid as per the abovementioned equations is defined in Eq. [10]

$$\mathbf{S}=\mu(\dot{\gamma})^{m-1}\dot{\Upsilon}, \tag{4}$$

where μ is the characteristics of each polymer and

$$\dot{\gamma}=\sqrt{\frac{1}{2}\sum_{i}\sum_{j}\dot{\gamma}_{ij}\dot{\gamma}_{ji}}\,,$$

where $\dot{\gamma}_{ij}$ $i,j=1,2,3$ is the rate of strain tensor component and

$$\dot{\Upsilon}=\mathbf{L}+\mathbf{L}^{\mathbf{T}}. \tag{5}$$

The expression that describe the geometry of the constricted portion of the tube is shown in Fig. 1.

$$h(z)=d(z)\left[1-\eta\left(b^{n-1}(z-a)-(z-a)^{n}\right)\right],\quad a\le z\le a+b, \tag{6}$$

$$=d(z),\qquad\qquad Otherwise$$

with

$$d(z)=d_0+\zeta^{*}z. \tag{7}$$

In the abovementioned equations, $\zeta^* = tan\phi$ which is called the tapering parameter, a is the length of the non-stenotic section, b is the length of the stenotic region, d_0 is the radius of the non-tapered artery in the non-stenotic part and n is a parameter that determines the shape of the constriction profile. For $n = 2$, the stenosis is symmetric. The parameter η is defined as

$$\eta = \frac{\delta n^{\frac{n}{(n-1)}}}{d_0 b^n (n-1)}, \tag{8}$$

where δ indicates the maximum height of the stenosis located at

$$z = a + \frac{b}{n^{\frac{1}{(n-1)}}}.$$

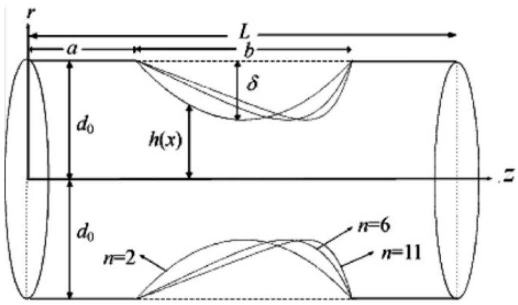

Fig. 1 Geometry of non-symmetric stenotic artery.

Now we present a detailed derivation of the governing equation for flow under consideration. For the flow under consideration,

$$\mathbf{V} = \Big[u(r,z), 0, w(r,z)\Big]. \tag{9}$$

Thus,

$$\mathbf{L} = \nabla\mathbf{V} = \begin{bmatrix} u_r & 0 & u_z \\ 0 & \frac{u}{r} & 0 \\ w_r & 0 & w_z \end{bmatrix}$$

and

$$\mathbf{L}^T = \begin{bmatrix} u_r & 0 & w_r \\ 0 & \frac{u}{r} & 0 \\ u_z & 0 & w_z \end{bmatrix}$$

with the subindex denoting differentiation with respect to the indicated variable.
Using the definition of the rate of strain tensor, we can write

$$\dot{\Upsilon} = \mathbf{L} + \mathbf{L}^T = \begin{bmatrix} 2u_r & 0 & u_z + w_r \\ 0 & \frac{2u}{r} & 0 \\ w_r + u_z & 0 & 2w_z \end{bmatrix}. \tag{10}$$

Now

$$\dot{\gamma} = |\dot{\Upsilon}| = \sqrt{\frac{1}{2}\sum_i \sum_j \dot{\gamma}_{ij}\dot{\gamma}_{ji}}\,,$$

and expanding the double sum we get

$$\dot{\gamma} = \left[\frac{1}{2}\Big(\dot{\gamma}_{11}\dot{\gamma}_{11} + \dot{\gamma}_{12}\dot{\gamma}_{12} + \dot{\gamma}_{13}\dot{\gamma}_{13} + \dot{\gamma}_{21}\dot{\gamma}_{21} + \dot{\gamma}_{22}\dot{\gamma}_{22} + \dot{\gamma}_{23}\dot{\gamma}_{23} + \dot{\gamma}_{31}\dot{\gamma}_{31} + \dot{\gamma}_{32}\dot{\gamma}_{32} + \dot{\gamma}_{33}\dot{\gamma}_{33}\Big)\right]^{\frac{1}{2}}.$$

Using the values of components of $\dot{\gamma}$ from Eq. (10) results in

$$\dot{\gamma} = \left[2u_r^2 + (u_z + w_r)^2 + 2\frac{u^2}{r^2} + 2w_z^2\right]^{\frac{1}{2}}. \tag{11}$$

Let us substitute for convenience

$$\dot{\gamma} = M. \tag{12}$$

From Eqs. (4), (10) and (12) the components of extra stress tensor for power law fluid can be written as

$$S_{rr} = 2\mu M u_r,\ S_{rz} = \mu M(u_z + w_r) = S_{zr},\ S_{\theta\theta} = 2\mu M\frac{u}{r}S_{zz} = 2\mu M w_z. \tag{13}$$

At this point, we make the assumption that stenosis is mild, i.e.

$$\frac{\delta}{d_0} << 1.$$

This assumption enables us to write

$$u = 0 \qquad and \qquad \frac{\partial u}{\partial z} = 0. \tag{14}$$

In view of Eq. (14), we can write

$$\dot{\gamma} = \sqrt{\left(\frac{\partial w}{\partial r}\right)^2} = \pm\frac{\partial w}{\partial r}. \tag{15}$$

The definition of magnitude requires the result to be a positive number. Thus, our choice of the sign that precedes $\left(\frac{\partial w}{\partial r}\right)$ in Eq. (15) depends on whether the derivative $\left(\frac{\partial w}{\partial r}\right)$ is positive or negative. Since the velocity is highest at the centre of the tube, thus, w is a decreasing function of r; therefore, $\left(\frac{\partial w}{\partial r}\right)$ is negative. Thus, the correct sign in Eq. (15) is negative: However Nadeem et al. [14] missed this point and blindly chose a positive sign preceding $\left(\frac{\partial w}{\partial r}\right)$ in Eq. (15) which is given by

$$\dot{\gamma} = -\left(\frac{\partial w}{\partial r}\right) > 0. \tag{16}$$

With the help of Eqs. (15) and (16), the components of stress and governing equations (1)–(3) reduce to

$$S_{rr} = 0, \qquad S_{\theta\theta} = 0, \qquad S_{zz} = 0,$$

$$S_{rz} = \mu\left(-\frac{\partial w}{\partial r}\right)^{m-1}\left(\frac{\partial w}{\partial r}\right) = S_{zr},$$

$$\frac{\partial p}{\partial r} = 0, \tag{17}$$

$$\frac{\partial p}{\partial z}=\frac{\mu}{r}\frac{\partial}{\partial r}\left[r\Big(-\frac{\partial w}{\partial r}\Big)^{m-1}\frac{\partial w}{\partial r}\right], \tag{18}$$

$$\frac{\partial u}{\partial r}+\frac{u}{r}+\frac{\partial w}{\partial z}=0. \tag{19}$$

To make the governing equations non-dimensional, we introduce the following dimensionless variables

$$\bar{r}=\frac{r}{d_0},\bar{z}=\frac{z}{b},\bar{w}=\frac{w}{u_0},\bar{h}=\frac{h}{d_0},\bar{u}=\frac{bu}{u_0\delta},\bar{p}=\frac{d_0^{m+1}p}{u_0^m b\mu},$$
$$R_e=\frac{\rho d_0^{m+1}}{u_0^{m-2}\mu b},\bar{S_{rr}}=\frac{bS_{rr}}{u_0^m\mu},\bar{S_{rz}}=\frac{d_0^m S_{rz}}{u_0^m\mu},\bar{S_{zz}}=\frac{bS_{zz}}{u_0^m\mu},\bar{S_{\theta\theta}}=\frac{bS_{\theta\theta}}{u_0^m\mu}, \tag{20}$$

where u_0 is the averaged velocity over the region of the tube with width d_0. Hence, the governing equations in non-dimensional form after dropping the bars read

$$\frac{\partial u}{\partial r}+\frac{u}{r}+\frac{\partial w}{\partial z}=0, \tag{21}$$

$$\frac{\partial p}{\partial r}=0, \tag{22}$$

$$\frac{\partial p}{\partial z}=\frac{1}{r}\frac{\partial}{\partial r}\left[r\Big(\frac{\partial w}{\partial r}\Big)^{m-1}\frac{\partial w}{\partial r}\right]. \tag{23}$$

The appropriate boundary conditions are

$$w=0 \qquad at \qquad r=h(z), \tag{24}$$

$$\frac{\partial w}{\partial r}=0 \qquad at \qquad r=0, \tag{25}$$

where

$$h(z)=(1+\xi z)\Big[1-\eta_1(z-\sigma)-(z-\sigma)^n\Big],\quad \sigma\le z\le\sigma+1,$$
$$\eta_1=\frac{\delta^* n^{\frac{n}{n-1}}}{n-1},\quad \delta^*=\frac{\delta}{d_0},\quad \sigma=\frac{a}{b},\quad \xi=\frac{\xi^* b}{d_0}.$$

The parameter $\xi(=tan\phi)$ is called the tapering parameter, and ϕ is known as the tapered angle. For the diverging tapering ($\phi>0$), converging tapering ($\phi<0$), non-tapered artery ($\phi=0$) (Fig. 2).

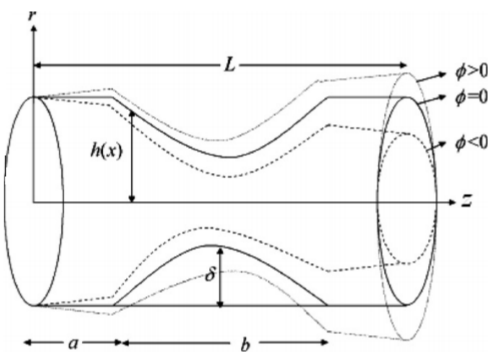

Fig. 2 Stenotic tapered artery for different taper angles.

3 Exact solution of the problem

Now we proceed to solve Eq. (23) subject to boundary conditions (24) and (25).
From Eq. (23), we can write

$$r\frac{\partial p}{\partial z} = \frac{\partial}{\partial r}\left[r\left(\frac{\partial w}{\partial r}\right)^m(-1)^{m-1}\right].$$

Integration of the abovementioned equation yields

$$\frac{r^2}{2}\frac{\partial p}{\partial z} + C = r\left(\frac{\partial w}{\partial r}\right)^m(-1)^{m-1}.$$

The boundary condition (Eq. 25) gives $C = 0$.
Thus, the abovementioned equation becomes

$$\frac{r^2}{2}\frac{\partial p}{\partial z} = r\left(\frac{\partial w}{\partial r}\right)^m(-1)^m(-1). \tag{26}$$

Now without giving the detail of algebra involved, we can write

$$\frac{\partial w}{\partial r} = \left(\frac{r}{2}\right)^{\frac{1}{m}}\frac{\partial p}{\partial z}\left|\frac{\partial p}{\partial z}\right|^{\frac{1}{m}-1}.$$

Integration of the abovementioned equation gives

$$w = \frac{1 r^{\frac{1}{m}+1}}{2^{\frac{1}{m}}\left(\frac{1}{m}+1\right)}\frac{\partial p}{\partial z}\left|\frac{\partial p}{\partial z}\right|^{\frac{1}{m}-1} + C_1. \tag{27}$$

From boundary conditions (Eq. 24), we get

$$C_1 = -\frac{1 h^{\frac{1}{m}+1}}{2^{\frac{1}{m}}\left(\frac{1}{m}+1\right)}\frac{\partial p}{\partial z}\left|\frac{\partial p}{\partial z}\right|^{\frac{1}{m}-1}, \tag{28}$$

and thus finally

$$w = \frac{\partial p}{\partial z}\left|\frac{\partial p}{\partial z}\right|^{\frac{1-m}{m}}\frac{m}{2^{\frac{1}{m}}(1+m)}\left[r^{\frac{m+1}{m}} - h^{\frac{m+1}{m}}\right], \tag{29}$$

$$F = 2\pi\int_0^h rw\,dr.$$

By substituting Eq. (29) in the definition of flow rate, we can write

$$F = \int_0^h A\left\{r.r^{\frac{m+1}{m}} - r.h^{\frac{m+1}{m}}\right\}dr, \tag{30}$$

where

$$A = 2\pi\frac{\partial p}{\partial z}\left|\frac{\partial p}{\partial z}\right|^{\frac{1-m}{m}}\frac{m}{2^{\frac{1}{m}}(1+m)}.$$

From Eq. (30), after some manipulation, we get

$$\frac{\partial p}{\partial z} = -\left(\frac{3m+1}{m}\right)\frac{h^{-(3m+1)}4F}{(2\pi)^m}\left(\frac{3m+1}{m}\right)h^{-(3m+1)}2F|^{m-1}. \tag{31}$$

The pressure drop is given by the following equation [11]:

$$\Delta p = \int_0^{\frac{L}{b}} \Big(-\frac{dp}{dz}\Big) dz. \tag{32}$$

Similarly, resistance–impedance is given by the following equation [11]

$$\lambda = \frac{\Delta p}{F} = \left\{ \int_0^{\frac{a}{b}} R(z)|_{h=1+\xi z}\, dz + \int_{\frac{a}{b}}^{\frac{a}{b}+1} R(z) dz + \int_{\frac{a}{b}+1}^{\frac{L}{b}} R(z)|_{h=1+\xi z} dz \right\}, \tag{33}$$

where

$$R(z) = \Big(\frac{3m+1}{m}\Big) \frac{h^{-\frac{3m+1}{m}} 4F}{(2\pi)^m} \Big(2\frac{3m+1}{m}\Big) h^{-\frac{3m+1}{m}} F|^{m-1}.$$

The non-dimensional shear stress is defined as

$$S_{rz} = -\Big(\frac{\partial w}{\partial r}\Big)^{m-1} \frac{\partial w}{\partial r}. \tag{34}$$

From Eq. (34), the wall stress can be obtained as

$$S_{rz}|_{r=h} = |\frac{\partial w}{\partial r}|^{m-1} \frac{\partial w}{\partial r}|_{r=h}. \tag{35}$$

Now since

$$\Big(\frac{\partial w}{\partial r}\Big)^{m-1} \frac{\partial w}{\partial r} = \frac{r}{2}\Big(\frac{\partial p}{\partial z}\Big),$$

therefore

$$S_{rz} = \frac{h}{2(2\pi)^m} \left[-\Big(\frac{3m+1}{m}\Big) h^{-\frac{3m+1}{m}} 4F \Big(\frac{3m+1}{m}\Big) h^{-\frac{3m+1}{m}} 2F|^{m-1} \right] \tag{36}$$

and

$$S_{rz}|_{r=h} = \frac{h}{2(2\pi)^m} \left[-\Big(\frac{3m+1}{m}\Big) h^{-\frac{3m+1}{m}} 4F \Big(\frac{3m+1}{m}\Big) h^{-\frac{3m+1}{m}} 2F|^{m-1} \right]. \tag{37}$$

Similarly, wall shear stress at maximum height of the stenosis, i.e. $h = 1-\delta$ is

$$\tau_s = S_{rz}|_{h=(1-\delta)} = \frac{(1-\delta)}{2(2\pi)^m} \left[-\Big(\frac{3m+1}{m}\Big)(1-\delta)^{-\frac{3m+1}{m}} 4F \Big(\frac{3m+1}{m}\Big)(1-\delta)^{-\frac{3m+1}{m}} 2F|^{m-1} \right]. \tag{38}$$

4 Results and discussion

In this section, the behaviour of flow quantities such as velocity profile, wall shear stress, shear stress at stenotic throat and resistance–impedance is displayed graphically for different values of the involved parameters. Figure 3 illustrates the effects of power law index m on velocity profile w in the stenotic region. This figure indicates an increase in w by increasing m. Thus, a fluid that exhibits shear thinning behaviour $(m < 1)$ flows slowly compared to Newtonian $(m = 1)$ and shear-thickening $(m > 1)$ fluids.

The effect of the severity of stenosis on the velocity profile w is shown in Fig. 4. We can see from this figure that for a fixed value of prescribed flux F, the velocity profile w increases near the centre, while it decreases near the wall with an increase in the severity of stenosis. The parameter ξ as defined earlier controls the degree of taperness of artery. For non-tapered artery, $\xi = 0$ while $\xi > 0$ and $\xi < 0$ correspond to diverging and converging artery, respectively. The effect of ξ on w can be observed from Fig. 5. Here, we note a decrease in w by increasing ξ . The parameter n that controls the shape of stenosis affects the velocity profile w in a similar way as ξ does. Wall shear stress S_{rz} profiles for different values of n, δ, m and ξ are shown in Figs. 7–10. Figures 11–13 are plotted to see the influence of n, m and ξ on resistance–impedance, while Figs. 14 and 15 depict the effect of m and F on shear stress at maximum height of the stenosis τ_s.

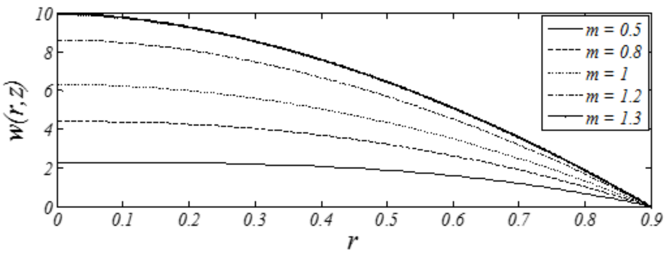

Fig. 3 Velocity variation for F=2, δ=0.4, n=2, a=0.2, b=0.4.

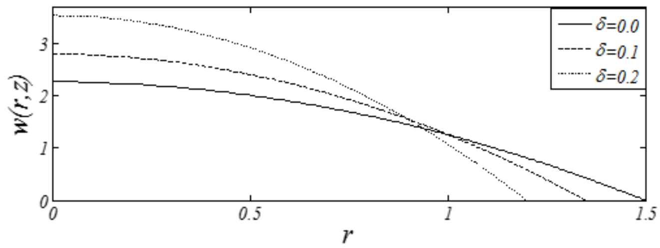

Fig. 4 Velocity variation for F=2, n=2, a=0.2, b=0.4, m=1.1.

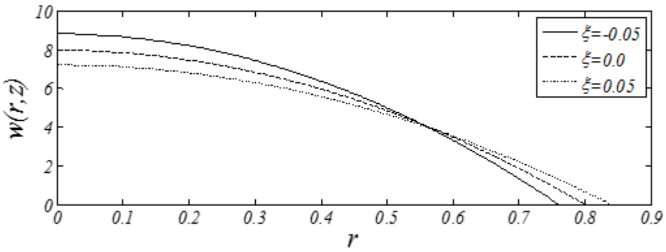

Fig. 5 Velocity variation for F=2,δ =0.2, n=2, a=0.2, b=0.4, m=1.

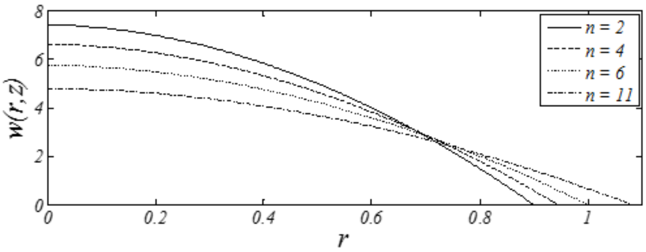

Fig. 6 Velocity variation for F=2, δ=0.4, a=0.2, b=0.4, m=1.1.

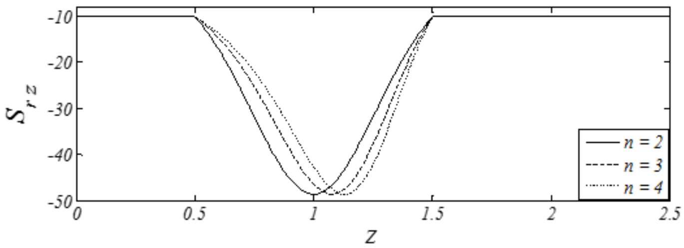

Fig. 7 Wall shear stress variation for F=1, δ=0.2, a=0.2, b=0.4, m=1.

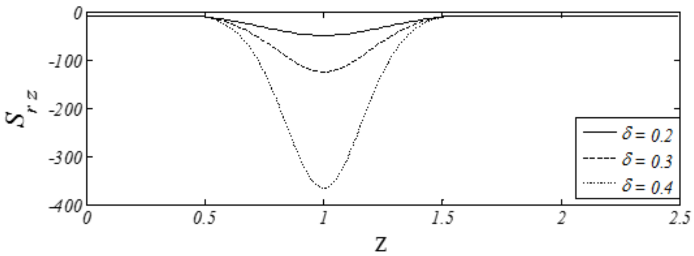

Fig. 8 Wall shear stress variation for F=1, L=1, a=0.2, b=0.4, m=1.

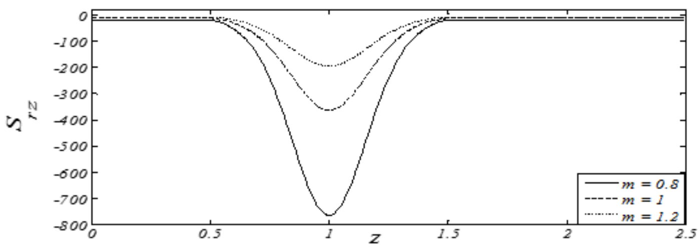

Fig. 9 Wall shear stress variation for F=1, L=1, a=0.2, b=0.4,δ=0.4.

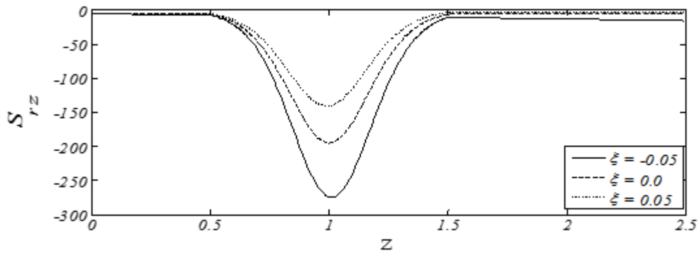

Fig. 10 Wall shear stress variation for F=1, L=1, a=0.2, b=0.4,δ=0.4.

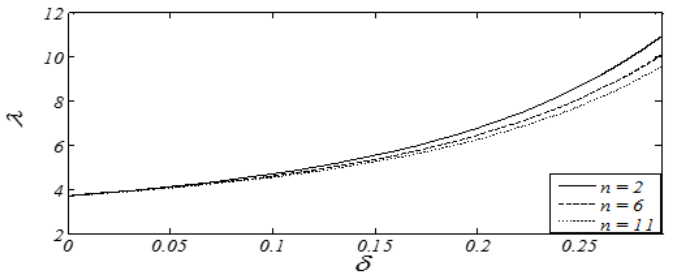

Fig. 11 Resistance impedance for F=0.6, L=1, a=0.2, b=0.4, m=2.

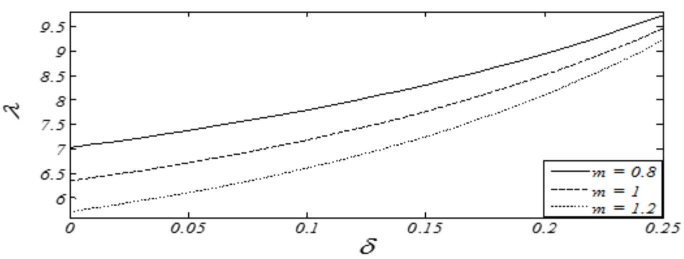

Fig. 12 Resistance impedance for F=0.6, L=1, a=0.2, b=0.4, n=2.

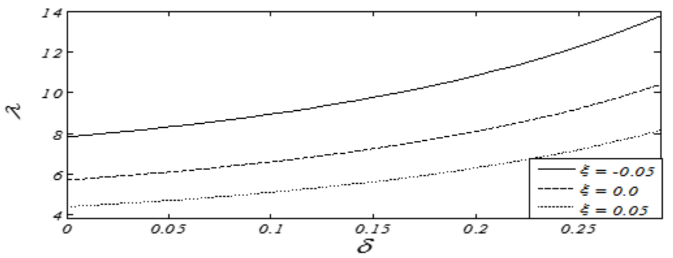

Fig. 13 Resistance impedance for F=0.6, L=1, a=0.2, b=0.4, m=1.2, n=2.

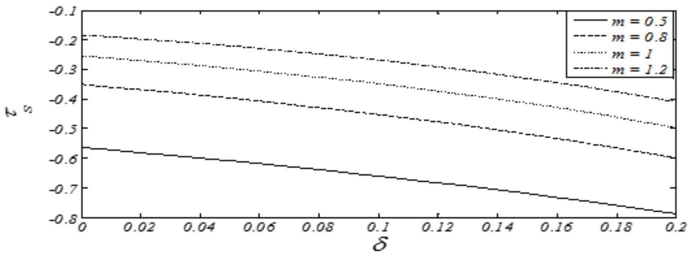

Fig. 14 Shear stress at stenotic throat for F=0.2.

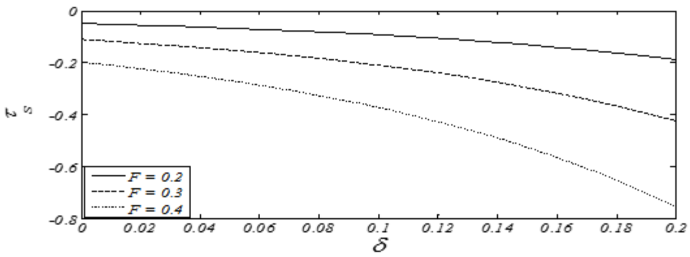

Fig. 15 Shear stress at stenotic throat for m=2.

The following observations can be made from Figs. 7 to 15.

Wall shear stress is symmetric for $n = 2$. However, it gets asymmetric otherwise. Its magnitude decreases with an increase in ξ and m. However, the situation becomes opposite with an increase in δ. The resistance impedance λ decreases by increasing m and ξ. The magnitude of shear stress at stenotic throat decreases by increasing m while it shows the opposite trend when m is fixed and F is increased.

Now at the end, we would like to mention that the results presented here for various flow features differ from those of Nadeem et al. [14] in many ways. A complete comparison of these results with ours is not of much interest to the reader and we therefore only present such comparison for results of velocity profile. Nadeem et al. [14] showed in their analysis (Fig. 5 page 7112) that for a prescribed positive flux velocity profile is negative over the whole cross-section $[0,h]$ in the stenotic region which if assumed true suggests that there is no flow in positive axial direction and whole fluid is moving backward. This result is self-contradictory because for prescribed positive flux the velocity profile over the whole cross-section could not be negative. Moreover, the presence of mild stenosis rather altering the direction of flow can alter only the speed of flow. Reverse flow is only possible if there is complete occlusion. On the contrary, our analysis (Fig. 3) shows that the flow speed in a normal artery is less than that of stenotic artery. There is no indication of reverse flow in our results.

5 Concluding remarks

An exact solution of governing equation for steady flow of a power law fluid through a tapered non-symmetric stenotic tube is obtained. The same problem was already addressed by Nadeem et al. [14], but the results presented by them were erroneous because of an incorrect choice of sign preceding the magnitude of the rate of deformation tensor appearing in the constitutive equation of power law fluid. Using the corrected solution, we have presented the graphical results for velocity profile, resistance–impedance and shear stress. Some discussion about these results is presented. Moreover, the difference between our velocity profile and the one obtained by Nadeem et al. [14] is also highlighted.

Acknowledgments

The research is supported by the National Basic Research Program of China (973 Program, Grant No. 2012CB026002) and the National Natural Science Foundation of China (Grant No.51775437).

References

[1] E. Rindfleish, Manual of Pathological Histology, *New Syndenham Soc, London*, 250(1) (1972), pp. 137–143.
[2] M. Nazemi, C. Kliestreuer, J. P. Archie and F. Y. Sorrell, Fluid flow and plaque formation in an aortic formation, *ASME J. Biomech. Eng.*, 111 (1989), pp. 316–324.
[3] C. G. Caro, J. M. Fitzerald and R.C. Shroter, Atheroma and arterial wall: shear observations, correlations and proposal of a shear dependent mass transfer mechanism for atherogeneses, *ProcR.Soc. Lond Set B*, 177 (1971), pp. 109–159.
[4] D.L. Fry, Certain histological and chemical responses to the vascular interface of acutely induced mechanical stress in the aorta of dog, *Circ Res, 24*, (1969), pp. 93–108.
[5] D.L. Fry, Responses of the arterial wall to certain physical fractions atherosclerosis initiating factors, *Associated Scientific Publishers, Amsterdam*, (Eds: R. Porterand J. Knight), (1973), pp. 93–125.
[6] P. N. Tandon, U. V. S. Rana, M. Kawahara and V. K. Katiyar, A model for blood flow through a stenotic tube,*Int J. Biomed Comput.*, 32 (1993), pp. 61–78.
[7] P. K. Mandal, Unsteady analysis of non-Newtonian blood flow through tapered arteries with a stenosis, *Int. J. Non-Linear Mech.*, 40 (2005), pp. 151–164.
[8] Md. A. Ikbal, S. Chakravarty, K. K. L. Wong, J. Mazumdar and P. K. Mandal, Unsteady response of non-Newtonian blood flow through a stenosed artery in magnetic field, *J.Comput.Appl.Math.*, 230 (2009), pp. 243–259.
[9] Z. Ismail, I. Abdullah, N. Mustapha and N. Amin, The power law model of blood flow through a tapered overlapping stenosed artery, *Appl. Math. Comput.*, 195 (2008), pp. 669–680.
[10] Kh. S. Mekheimer and M. A. Elkot, The micropolar fluid model for blood flow through a tapered artery with a stenosis, *Acta Mech.Sin.*, 24 (2008), pp. 637–644.
[11] I. Abdullah, N. Amin, A micropolar fluid model of blood flow through a tapered artery with a stenosis, *Math. Meth. Appl. Sci.*, 33 (2010), pp. 1910–1923.
[12] Kh. S. Mekheimer and M. A. Elkot, Mathematical modeling of unsteady flow of a Sisko fluid through anisotropically tapered elastic arteries with time-variant overlapping stenosis, *App.Math.model*, 36 (2012), pp. 5393–5407.
[13] D. S. Sankar, and U. Lee, Mathematical modeling of pulsatile flow of non-Newtonian fluid in stenosed arteries, *Commun. Nonlinear Sci. Numer. Simul.*, 14 (2009), pp. 2971–2981.
[14] S. Nadeem, Noreen Sher Akbar, A. A. Hendi and T. Hayat, Power law fluid model for blood flow through a tapered artery with a stenosis, *App.Math.comp.*, 217(17) (2011), pp. 7108–7116.